

HEMODYNAMICALLY NON-SIGNIFICANT CORONARY ARTERY STENOSIS: A PREDICTIVE MODEL

Gaudio L.T.^(a), De Rosa S.^(b), Indolfi C.^(c), Caruso M.V.^(d), Fragomeni G.^(e)

^(a,d,e)Bioengineering Unit, Department of Medical and Surgical Sciences, Magna Graecia University, Catanzaro
^(b,c)Cardiology Unit, Department of Medical and Surgical Sciences, Magna Graecia University, Catanzaro

^(a)l.gaudio@unicz.it, ^(b)saderosa@unicz.it, ^(c)indolfi@unicz.it, ^(d)mv.caruso@unicz.it, ^(e)fragomeni@unicz.it

ABSTRACT

Coronary artery disease (CAD), which is characterized by the presence of coronary artery stenosis, is the frequent cause of death worldwide. The aim of this study was to assess hemodynamic effect due to the presence of non critical coronary stenoses. The computational fluid dynamics (CFD) was used to carry out numerical simulations, investigating the hemodynamic parameters. Twenty-four stenotic coronary arteries, with different non-significant stenosis severities, were reconstructed from frames of coronary angiographies of patients. The results show the distribution of the wall shear stress (WSS) in coronary vessels, and will be used to develop a predictive model to obtain shear stress value knowing stenosis area and length.

These models demonstrate that the assessment of WSS parameters may be useful to further refine risk stratification of patients having not clinically significant coronary artery stenosis.

Keywords: stenosis, computational fluid dynamics (CFD), wall shear stress (WSS), predictive models

1. INTRODUCTION

Coronary artery disease (CAD) is the most widely recognized cause of death. The number of deaths due to CAD has substantially increased between 1990 and 2013, rising from 5.74 million (12%) deaths to 8.14 million deaths (16.8%) (Nagavi 2015).

In 2015, 281,364 coronary angiography exams were performed in Italy, and during about the 50% of these examinations some revascularization procedures were needed. (Berti 2015)

Two main features of coronary stenosis are: the reduction of the section (i.e. the caliber of the lumen of the vessel) and the reduction of the diameter in the longitudinal direction (Falk 1995).

A stenosis is defined as hemodynamically significant when it reduces the diameter of a coronary vessel for at least 50% (Chang 2000).

Numerous trials have shown that the majority of coronary thromboses occurs on a non-obstructive plaque and often from plaques with mild stenosis (Pavone 2008).

Indeed, myocardial infarction is often the result of the rupture of a vulnerable plaque that does not determine any reduction of the coronary lumen (Pavone 2008).

Through some techniques, such as computational fluid dynamics (CFD), it is possible to solve basic equations that model the flow movement in different conditions and to calculate not easily accessible parameters in silico (Mazzitelli 2016).

Many advantages of CFD reside in the possibility to analyze different problems in different conditions. The level of detail is practically unlimited and repeatable (Steinman 2002).

Therefore, a study of the WSS focused on the onset of a coronary plaque and on plaque vulnerability can provide useful information to stratify patients at risk of adverse events (Eshtehardi 2016).

For this reason, many studies have been conducted by CFD analysis to investigate the hemodynamic variables involved in presence of stenosis of the coronary arteries (Caruso 2015).

Many authors have focused their analysis only on significant stenosis, consequently a detailed analysis of what happens in the presence of not significant stenosis is needed (Chaicana 2012) (Chaicana 2014) (Papadopoulos 2016).

The present study was conducted by including patients with non-significant stenosis for the purpose of evaluating changes of the hemodynamic parameters for different degrees of stenosis with the aim of developing a predictive model. The purpose of the model is to make a prediction of the WSS value by knowing the percentage area and stenosis length to support decisions in the medical-clinical setting.

2. MATERIAL AND METHODS

In this study, a cohort of 24 patients was considered.

All of the patients had a hemodynamically non-significant stenosis.

2.1 Geometry Reconstruction

For each coronary vessel, the geometry was reconstructed starting from a series of angiograms acquired during standard x-ray angiographies. The angiographic frame corresponding to the end of the diastole was selected to avoid any impact of systole on vessel geometry.

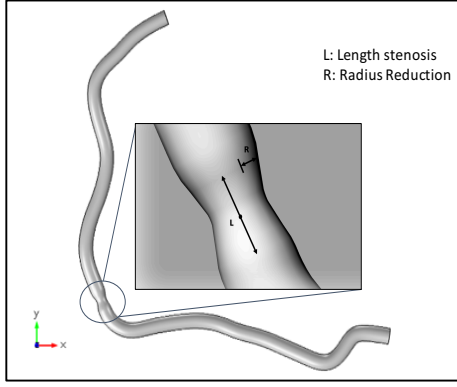


Figure 1: Coronary artery reconstruction

Geometry models were reconstructed using RHINOCEROS v.4.0 software (Robert McNeel & Associates, Seattle, WA, USA).

Figure 1 shows the geometrical model considered: the coronary of each patient incorporates the proximal section, the central section with stenoses and the distal one. It is considered in this study stenosis appeared on the main branch, as for all patients.

The evaluation of the stenosis percentage is obtained from the ratio between the minimum diameter of the lumen at the narrowest point level of the lesion and the reference diameter, which is the average of the lumen diameters in the reference segments upstream and downstream from the stenosis, judged as apparently healthy (Falk 1995).

From these parameters the percentage of the stenosis area was calculated as the ratio between the area of the healthy vessel ($Area_n$) and the area in the presence of stenosis ($Area_s$):

$$Area\% = \frac{Area_s}{Area_n} \cdot 100 \quad (1)$$

The length of stenosis for each patient was considered.

2.2 CFD Analysis

The software used to perform the simulations was COMSOL Multiphysics 5.2 (COMSOL Inc., Stockholm, Sweden). In the study, the blood was assumed as Newtonian with a density of $1.050 [Kg/m^3]$ and viscosity of $0.0045 [Pa \cdot s]$ (Stalder 2011).

The flow was considered as laminar, and 3D Navier-Stokes equations were used as governing laws (Gramigna 2015).

The incompressible condition gives:

$$\nabla \cdot \mathbf{u} = 0 \quad (2)$$

The governing equation used to solve the laminar model is:

$$\rho \frac{\delta \mathbf{u}}{\delta t} + \rho (\mathbf{u} \cdot \nabla) \mathbf{u} = \nabla \cdot \{-p\mathbf{I} + \mu[\nabla \mathbf{u} + (\nabla \mathbf{u})^T]\} \quad (3)$$

where ρ is the fluid density, \mathbf{u} is the fluid velocity, p is the pressure, \mathbf{I} is the unit diagonal matrix and μ is the viscosity (Caruso 2016).

For each patient, a time-dependent flow waveform was assumed as an inlet boundary condition and as an outlet condition a specific waveform pressure was applied for each patient. All data and images used are specific to each patient, acquired after obtaining informed consent. The no-slip boundary condition was applied to the wall to assume that the fluid in contact with walls is zero velocity (Caruso 2017).

Then the domain was discretized with tetrahedral and prismatic element, as shown in Figure 2, with an amount of $\sim 205,000$ elements for each coronary artery model.

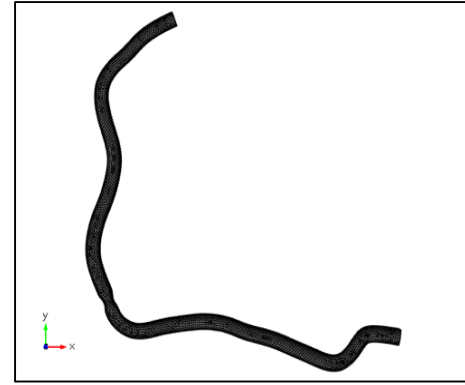


Figure 2: Coronary artery mesh

A comparison was made between two meshes. Table 1 shows the domain element statistics on the two mesh. For this geometry a finer mesh was chosen for better average element quality and a major number of elements.

Table 1: Finite Element Mesh

Domain Element Statistic		
Mesh Type	Finer	Fine
Number of elements	291662	80738
Average element quality	0,623	0,602
Mesh volume [mm^3]	1356	1342

Steady-state and transient CFD computations were performed; for the steady state and the time-dependent computation the PARDISO direct solver was used.

The index responsible for the change of morphology was calculated together with the orientation of the tissue that constitutes the wall of blood vessels: the wall shear stress (WSS) (Caruso 2015). That is defined by:

$$WSS = \sqrt{(\tau_x)^2 + (\tau_y)^2 + (\tau_z)^2} \quad (4)$$

where τ_x, τ_y, τ_z are the viscous stresses in x, y, z directions, respectively.

WSS values less than $1 N/m^2$ mean the developing of plaque progression (Samady 2011).

WSS values greater than 3 N/m^2 are in the region of stenosis and involve clotting referred to the intimal thickness (Dolan 2014).

3. RESULTS

3.1. CFD RESULTS

The CFD results of 24 coronary arteries having a non-significant stenosis showed the distribution of the blood flow.

To represent the fluid dynamics within the 24 vessels under study, it was decided to show the results of the simulations of only one patients.

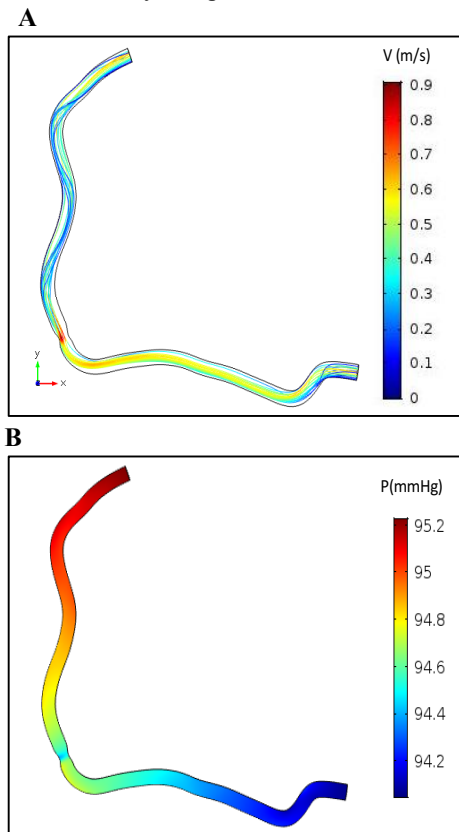


Figure 3: Coronary artery's A) velocity streamlines B) pressure

Figure 3A shows streamlines at the systolic peak to visually describe the fluid flow. The color expression in the streamlined plot indicates velocity magnitude (in $[m/s]$).

As shown in Figure 3A there is an increasing speed in correspondence to the lumen restriction where the maximum value of 0.9 [m/s] is reached.

Figure 3B shows the distribution of pressure; it is noted that the distal pressure due to the presence of the stenosis is less than the proximal pressure.

The WSS on the segment of stenosis was then calculated. Figure 4 shows the distribution of the WSS during the systolic peak in $[N/m^2]$. Its maximum value is reached along the stenosis of the coronary artery, that is, the maximum value occurs where there is a narrowing of the

vessel due to the presence of stenosis and this value is $1.89 \text{ [N/m}^2]$.

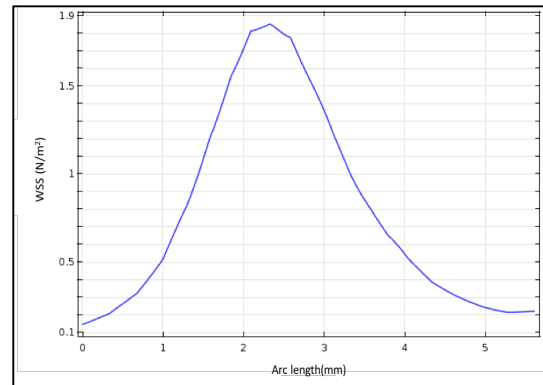


Figure 4: WSS value of the stenosis segment

The table 2 shows the overall results obtained from the CFD analysis of 24 patients. Patients were grouped into subgroups of 4 based on the percentage reduction of area due to stenosis. For each subgroup the mean length of the stenosis segment and the mean WSS was reported.

Table 2: Mean of results for 24 patients

	Range of Reduction Area [%]	Length Stenosis [mm]	WSS [Pa]
Group A	[2,11]	1,16	0,85
Group B	[12,22]	1,55	2,15
Group C	[23,34]	1,74	3,47
Group D	[36,60]	1,95	4,75

3.2. PREDICTION MODEL

For each patient, the data of the stenosis area - in percentage - and of the length of the stenosis have been reported.

Furthermore, for each model of coronary artery the average values of the wall shear stress calculated on a surface of 2 mm length above and below the central point of stenosis are reported.

The data were used to perform the fitting curves and obtain the surfaces shows in Figure 5A. A first degree polynomial function was applies:

$$WSS = -1.554 + 1.931 \text{ length} + 0.05484 \text{ area} \quad (5)$$

where the coefficients have 95% confidence bounds and R-square goodness of the fit is 0.9094.

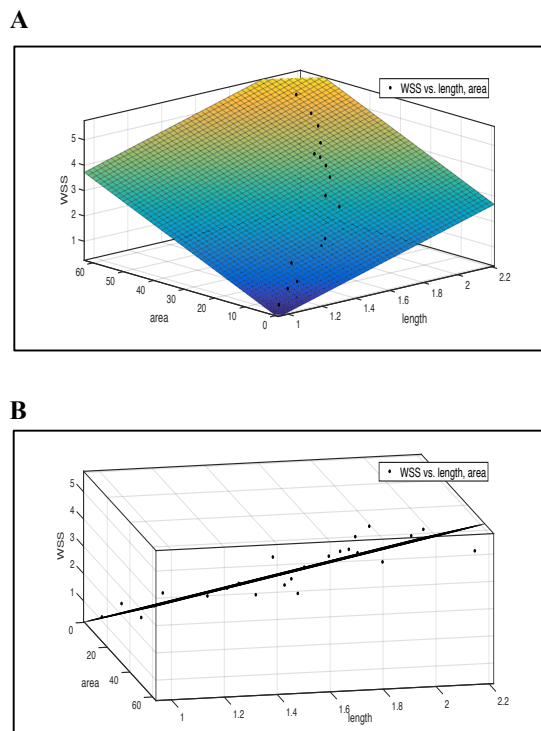


Figure 5: Model Prediction WSS vs Area, Length
A) surface B) interpolation line

4. DISCUSSION

CFD analyses were performed in order to obtain the numerical results affecting blood velocity and shear stress on the wall, starting from Finite Elements of coronaries reconstructed geometries.

The flow generated by the coronary models, as shown in Figure 3, has an asymmetrical distribution of velocity streamlines, tangent lines to the instantaneous velocity vectors of the flow, toward the stenosis. The blood flow reaches the maximum velocity value during systole, at time $t = 0.575$ sec.

This value, as shown in Figure 3, is equal to $0.9 [m/s]$ and occurs in correspondence to the narrowing of the vessel. As the degree of stenosis increases, i.e. the narrowing of the lumen of the vessel increases, the velocity increases. A high value of blood velocity downstream of the stenosis may cause turbulence phenomena. A raise of the velocity increases the tendency of red blood cells to accumulate in the axial laminae.

Wall shear stress (WSS) was finally analyzed. WSS assumes higher values where there is a narrowing of the vessel, and for the case of Figure 4 the maximum value is $1.89 [N/m^2]$.

Although, only in presence of significant stenosis, WSS reaches values of above $3 [N/m^2]$ in the region of stenosis, involving clotting referred to the intimal thickness (Dolan 2014).

In these areas, a chronic high WSS value not only stimulates adaptative outward remodeling but also

contributes to the saccular formation and atherosclerotic plaque destabilization (Souli 2004).

On the contrary, in some regions both upstream and downstream of the stenosis, a low WSS value results, and there may be oscillation of WSS and stagnation of fluid, inducing perturbed endothelial alignment (Samady 2011).

Therefore investigating this parameter could provide additional information about the development of atherosclerosis in the vessel. For this purpose the prediction model has been created, in order to provide a forecast of the wall shear stress mean value starting from the area percentage and from the length of stenosis.

Figure 5A shows the surface at different variations of color gradation, from areas with low values of WSS in blue to areas with high values in red. If the percentage of stenosis and the length of the stenotic tract increase, there is an increase of the wall shear stress.

In fact, as it can be seen in Figure 5A, for the critical areas and the critical lengths the average value of WSS increases and becomes greater than $3 [N/m^2]$.

Therefore that might be a useful indicator in order to stratify patients who, even if only treated with drug therapy, may undergo adverse events at follow-up.

5. CONCLUSION

This study showed that the inclusion of additional information on stenosis geometry allows a better stratification of patient's clinical risk, encompassing the predicted impact of flow parameters, such as the WSS despite the stenosis is non-significant.

To this purpose, the prediction of the wall shear stress can be useful to provide additional information about the progression of atherosclerotic plaque and endothelial damage and, consequently about the evolution of the disease.

6. LIMITATION AND FUTURE DIRECTIONS

A number of simplifying assumption were made to build up the model.

The first limitation of the study concerns the following simplifying assumption of rigid walls. Actually the blood vessels are distensible, since the area of the section of the vessel may changes as a function of vessel pressure. The second limitation is that blood is assumed as Newtonian. In presence of shear rate $>100/s$ the assumption is generally accepted the assumption but in smaller vessels it is necessary to consider the non-Newtonian effect (Formaggia 2009). Next steps, through the use of specific sensors, will be needed to validate the data.

Further studies are needed to investigate coronary arteries in presence of hemodynamically significant stenosis to implement a more detailed prediction model.

REFERENCES

- Berti S., Piccaluga E., Marchese A., Varbella F., Sardella G., Danzi G. B., and Magro B. 2015. Documento di posizione SICI-GISE sugli standard e linee guida per i laboratori di diagnostica e

- interventistica cardiovascolare. *Giornale Italiano di Cardiologia*, 16(10), 590-600.
- Caruso M. V., De Rosa S., Indolfi C., and Fragomeni G. 2015. Computational analysis of stenosis geometry effects on right coronary hemodynamics. In *Engineering in Medicine and Biology Society (EMBC), 2015 37th Annual International Conference of the IEEE* (pp. 981-984). IEEE.
- Caruso M. V., Gramigna V., Renzulli A., and Fragomeni, G. 2016. Computational analysis of aortic hemodynamics during total and partial extra-corporeal membrane oxygenation and intra-aortic balloon pump support. *Acta of Bioengineering and Biomechanics*, 18(3), 3-9.
- Caruso M. V., Renzulli A., and Fragomeni G. 2017. Influence of IABP-Induced Abdominal Occlusions on Aortic Hemodynamics: A Patient-Specific Computational Evaluation. *ASAIO Journal*, 63(2), 161-167.
- Chaichana T., Sun Z., and Jewkes J. 2012. Computational fluid dynamics analysis of the effect of plaques in the left coronary artery. *Computational and mathematical methods in medicine*, 2012.
- Chaichana T., Sun Z., and Jewkes J. 2013. Hemodynamic impacts of left coronary stenosis: A patient-specific analysis. *Acta of bioengineering and biomechanics*, 15(3).
- Chang J. B., Prasad K., and Olsen E. R. 2000. *Textbook of angiology*. Springer.
- Creager M. A., Beckman J. A., and Loscalzo J. 2012. *Vascular medicine: a companion to Braunwald's heart disease*. Elsevier Health Sciences.
- Dolan J. M., Kolega J., and Meng H. 2013. High wall shear stress and spatial gradients in vascular pathology: a review. *Annals of biomedical engineering*, 41(7), 1411-1427.
- Eshtehardi P., and Teng, Z. 2016. Protective or destructive: High wall shear stress and atherosclerosis. *Atherosclerosis*, 251, 501-503.
- Falk, E., Shah, P. K., and Fuster, V. 1995. Coronary plaque disruption. *Circulation*, 92(3), 657-671.
- Formaggia, L., Quarteroni, A., and Veneziani, A. (Eds.). 2010. *Cardiovascular Mathematics: Modeling and simulation of the circulatory system* (Vol. 1). Springer Science & Business Media.
- Gramigna V., Caruso M. V., Rossi M., Serraino G. F., Renzulli A., and Fragomeni G. 2015. A numerical analysis of the aortic blood flow pattern during pulsed cardiopulmonary bypass. *Computer methods in biomechanics and biomedical engineering*, 18(14), 1574-1581.
- Mazzitelli R., Boyle F., Murphy E., Renzulli A., and Fragomeni G. 2016. Numerical prediction of the effect of aortic Left Ventricular Assist Device outflow-graft anastomosis location. *Biocybernetics and Biomedical Engineering*, 36(2), 327-343.
- Naghavi M., Wang H., Lozano R., Davis A., Liang X., Zhou M., and Aziz, M. I. A. 2015. Global, regional, and national age-sex specific all-cause and cause-specific mortality for 240 causes of death, 1990-2013: a systematic analysis for the Global Burden of Disease Study 2013. *Lancet*, 385(9963), 117-171.
- Papadopoulos K. P., Gavaises M., Pantos I., Katritsis D. G., and Mitroglou N. 2016. Derivation of flow related risk indices for stenosed left anterior descending coronary arteries with the use of computer simulations. *Medical Engineering & Physics*, 38(9), 929-939.
- Samady H., Eshtehardi P., McDaniel M. C., Suo J., Dhawan S. S., Maynard C., and Giddens, D. P. 2011. Coronary artery wall shear stress is associated with progression and transformation of atherosclerotic plaque and arterial remodeling in patients with coronary artery disease. *Circulation*, CIRCULATIONAHA-111.
- Soulis J. V., Farmakis T. M., Giannoglou G. D., and Louridas G. E. 2006. Wall shear stress in normal left coronary artery tree. *Journal of biomechanics*, 39(4), 742-749.
- Stalder A. F., Liu Z., Hennig J., Korvink J. G., Li K. C., and Markl M. 2011. Patient specific hemodynamics: combined 4D flow-sensitive MRI and CFD. In *Computational Biomechanics for Medicine* (pp. 27-38). Springer New York.
- Steinman D. A. 2002. Image-based computational fluid dynamics modeling in realistic arterial geometries. *Annals of biomedical engineering*, 30(4), 483-497.